The relative thermodynamic stabilities of $^2Co_3(CO)_3(PMe_3)_6$ and $^1HCo_3(CO)_3(PMe_3)_6$ complexes may be connected by an equilibrium

$$^2H + {}^2Co_3(CO)_3(PMe_3)_6 \rightleftharpoons {}^1HCo_3(CO)_3(PMe_3)_6$$

Our results (Table IX) indicate that only the D model of $^1HCo_3(CO)_3(PMe_3)_6$ is significantly more stable than $^2Co_3(CO)_3(PMe_3)_6$.

Conclusions

Formation of triangulo clusters of cobalt and nickel in directed syntheses may be initiated photochemically or thermally depending on the reactants. For the heteronuclear species **2** a unique feature emerges: If two mononuclear complexes, **6** and **10**, each perfectly stable at room temperature, are brought together in a hydrocarbon solvent, they undergo a spontaneous condensation reaction to form the triangulo cluster exclusively.

1 and **2** are not cleaved by phosphine ligands and may be recrystallized without decomposition. However, a 46-electron count is maintained together with unsaturation and high reactivity. The structures of **1** and **2** show tight metal to metal bonds involving CoH or Ni fragments. **1** and **2** also serve to demonstrate the differences in chemical properties of two isoelectronic triangulo clusters.

1 appears to have a pseudo-D_{3h} core that is mainly held together by carbonyl bridges. If allowance is made for some out of plane CoH stretching, its center is the most probable hydrogen position. As a result of molecular dynamics such as hydrogen tunneling, the hydride ligand resides at both sides of the Co_3 triangle.

Acknowledgment. We thank the Fonds der Chemischen Industrie and the Deutsche Forschungsgemeinschaft for financial support of this work.

Supplementary Material Available: Listings of crystallographic details, atomic positional parameters, anisotropic thermal parameters, and hydrogen positional and thermal parameters for **1** and **2** (3 pages). Ordering information is given on any current masthead page.

OM9107193

Trinuclear and Dinuclear Fluorinated Ferroles by Cluster Rearrangement and Degradation Reactions

Dieter Lentz,* Heike Michael-Schulz, and Marion Reuter

Institut für Anorganische und Analytische Chemie der Freien Universität Berlin, Fabeckstrasse 34-36, D-1000 Berlin 33, FRG

Received March 19, 1992

Thermolysis of the diferraallyl clusters $Fe_3(CO)_8(\mu_3\text{-}CF)(\mu_3\text{-}CFCRCR')$ (**1a–d**) (**a**, R = R′ = H; **b**, R = R′ = CH_3; **c**, R = CH_3, R′ = C_6H_5; **d**, R = H, R′ = CH_3) in hexane yields the isomeric trinuclear ferroles $Fe_2(CO)_8(FeCFCRCR'CF)$ (**2a–d**) and $Fe_2(CO)_8(FeCFCFCRCR')$ (**3a–c**) and the corresponding dinuclear species $Fe(CO)_6(FeCFCRCR'CF)$ (**4a–d**) and $Fe(CO)_6(FeCFCFCRCR')$ (**5a–c**), respectively. The ratio of the products and small amounts of minor products depends on the substituents. The structures of $Fe_2(CO)_8(FeCFCHCHCF)$ (**2a**), $Fe_2(CO)_8(FeCFCFCHCH)$ (**3a**), and $Fe_2(CO)_8(FeCFCCH_3CC_6H_5CF)$ (**2c**) have been established by X-ray crystal structure determinations: **2a**, orthorhombic, *Pcab*, a = 11.416 (4) Å, b = 15.748 (4) Å, c = 16.129 (5) Å, R = 0.040, R_w = 0.040; **3a**, orthorhombic, *Pnma*, a = 11.524 (9) Å, b = 10.994 (9) Å, c = 11.42 (2) Å, R = 0.040, R_w = 0.041; **2c**, monoclinic, $P2_1/c$, a = 18..214 (6) Å, b = 7.035 (3) Å, c = 17.845 (6) Å, β = 117.37 (3)°, R = 0.105, R_w = 0.080.

Introduction

Ferroles have been first isolated and characterized among the complicated mixture of products obtained by the reaction of dodecacarbonyltriiron and alkynes.[1] Many dinuclear[2] and trinuclear[3] ferroles have been synthesized. However, only one fluorinated ferrole, which is formed in a unknown way from $Fe(CO)_5$ and $CFBr_3$,[4] has been reported thus far, whereas the second example[5] has proved to the erroneous.[6] Difluoroethyne cannot be used as a starting material due to its extreme instability,[7] and only two difluoroethyne complexes have been reported thus far, which have been prepared in an indirect way.[8]

Mathieu et al. reported the formation of ferroles on the thermal reaction of $Fe_3(CO)_9(\mu_3\text{-}CCH_3)$ ($\mu_3\text{-}COC_2H_5$) with alkynes.[9] The presence of several isomers has been explained by a complicated mechanism, which postulated the formation of intermediate diferraallyl clusters. However, on the photolytic reaction of $Fe_3(CO)_9(\mu_3\text{-}CF)_2$ with alkynes we obtained diferrallyl clusters in a very regioselective reaction.[10] In the single case of the phosphaalkyne $t\text{-}C_4H_9\text{–}C{\equiv}P$ a phosphaferrole type cluster was obtained.[11]

(1) Reppe, W.; Vetter, H. *Liebigs Ann. Chem.* **1953**, *582*, 133. Hübel, W.; Braye, E. H. *J. Inorg. Nucl. Chem.* **1959**, *10*, 250. Dodge, R. P.; Schomaker, V. *J. Organomet. Chem.* **1965**, *3*, 274. Hock, A. A.; Mills, O. S. *Acta Crystallogr.* **1961**, *14*, 139.

(2) Dettlaf, G.; Krüerke, U.; Kuhn, N.; Mirbach, M. In *Gmelin Handbuch der Anorganischen Chemie*; Springer-Verlag: Berlin, Heidelberg, New York, 1980; Fe Organoiron Compounds, Part C3. Fehlhammer, W. P.; Stolzenberg, H. In *Comprehensive Organometallic Chemistry*; Wilkinson, G., Ed.; Pergamon: Oxford, England, 1982; Vol 4.

(3) Mirbach, M.; Petz, W.; Siebert, C. Wilcke, B. In *Gmelin Handbook of Inorganic Chemistry*; Springer-Verlag: Berlin, Heidelberg, New York, Tokyo, 1987; Fe Organoiron Compounds, Part C7.

(4) Lentz, D.; Michael, H. *J. Organomet. Chem.* **1988**, *346*, C37.

(5) Mirkin, C. A.; Lu, K.-L.; Geoffroy, G. L.; Rheingold, A. L. *J. Am. Chem. Soc.* **1990**, *112*, 461.

(6) Mirkin, C. A.; Lu, K.-L.; Geoffroy, G. L.; Rheingold, A. L. *J. Am. Chem. Soc.* **1990**, *112*, 6155.

(7) Bürger, H.; Sommer, S. *J. Chem. Soc., Chem. Commun.* **1991**, 456.

(8) Lentz, D.; Michael, H. *Angew. Chem.* **1988**, *100*, 871; *Angew. Chem., Int. Ed. Engl.* **1988**, *27*, 845. Lentz, D., Preugschat, D. *Angew. Chem.* **1990**, *102*, 308; *Angew. Chem., Int. Ed. Engl.* **1990**, *29*, 315.

(9) Nuel, D.; Dahan, F.; Mathieu, R. *J. Am. Chem. Soc.* **1985**, *107*, 1658.

(10) Lentz, D.; Michael, H. *Chem. Ber.* **1988**, *121*, 1413. Lentz, D.; Michael, H. *Inorg. Chem.* **1990**, *29*, 4396.

(11) Lentz, D.; Michael, H. *Angew. Chem.* **1989**, *101*, 330; *Angew. Chem., Int. Ed. Engl.* **1989**, *28*, 321.

0276-7333/92/2311-2916$03.00/0

The trinuclear ferroles are closo clusters according to Wade's rules,[12] whereas the diferraallyl clusters are capped nido clusters. In continuation of our studies on the chemistry of iron clusters with fluorinated ligands, we have studied the thermolysis of the diferraallyl clusters $Fe_3(CO)_8(\mu_3\text{-CF})(\mu_3\text{-CF-CR-CR}')$ (**1a–d**) (**a**, R = R′ = H; **b**, R = R′ = CH_3; **c**, R = CH_3, R′ = C_6H_5; **d**, R = H, R′ = CH_3) in *n*-hexane in order to get information about the possibility of cluster rearrangement reactions.

Experimental Section

All reactions were carried out under dry argon by using standard Schlenk tube and vacuum techniques. ^1H NMR, ^{19}F NMR, and ^{13}C NMR spectra were recorded by using a Jeol FX 90Q instrument using TMS, $CFCl_3$, and TMS or solvent signals as reference standards. The product composition and isomeric ratio were monitored by TLC chromatography and, directly after filtration of the reaction mixture over silica to remove paramagnetic impurities, by ^{19}F NMR spectroscopy. Computer simulations of the NMR spectra were performed with the LAOCN3 program.[13] IR spectra were taken on a Perkin-Elmer 883 instrument. Mass spectra were obtained on a Varian 711 spectrometer (80 eV). $Fe_3(CO)_8(\mu_3\text{-CF})(\mu_3\text{-CF-CH-CH})$[10] (**1a**), $Fe_3(CO)_8(\mu_3\text{-CF})(\mu_3\text{-CFCCH}_3\text{CCH}_3)$[10] (**1b**), $Fe_3(CO)_8(\mu_3\text{-CF})(\mu_3\text{-CFCCH}_3\text{CC}_6\text{H}_5)$[10] (**1c**), and $Fe_3(CO)_8(\mu_3\text{-CF})(\mu_3\text{-CFCHCCH}_3)$[10] (**1d**) were prepared by literature methods.

$Fe_2(CO)_8$(FeCFCHCHCF) (2a), $Fe_2(CO)_8$(FeCFCFCHCH) (3a), $Fe(CO)_6$(FeCFCHCHCF) (4a), and $Fe(CO)_6$(FeCFCFCHCH) (5a). $Fe_3(CO)_8(\mu_3\text{-CF})(\mu_3\text{-CFCHCH})$ (**1a**) (250 mg, 0.52 mmol) was dissolved in *n*-hexane and sealed in a glass tube (4-mm outer diameter) under vacuum, and the contents were heated to 80 °C for 3 days. The reaction was monitored by ^{19}F NMR spectroscopy. After the glass tube was opened, the compounds were dissolved in a minimum amount of *n*-hexane. Separation of the products has been performed using a medium-pressure liquid chromatography column (l = 65 cm, d = 3.5 cm; silica 60, 0.015–0.040 mm) using light petroleum (bp 40–60 °C) as eluant. The first yellow fraction contains **5a**, the second one **4a**, the third one **3a**, and the fourth one **2a**. Crystallization yields **2a** (8 mg, 0.020 mmol), **3a** (10 mg, 0.021 mmol), **4a** (32 mg, 0.087 mmol), and **5a** (8 mg, 0.022 mmol), respectively.

$Fe_2(CO)_8$(FeCFCHCHCF) (2a): dark green crystals, mp 125 °C dec. MS [*m/e* (%, assignment)]: 480 (4, M^+), 452 (45, M^+ – CO), 424 (15, M^+ – 2CO), 396 (12, M^+ – 3CO), 368 (30, M^+ – 4CO), 340 (53, M^+ – 5CO), 312 (83, M^+ – 6CO), 284 (69, M^+ – 7CO), 256 (83, M^+ – 8CO), and smaller fragment ions.

$Fe_2(CO)_8$(FeCFCFCHCH) (3a): dark green crystals, mp 135 °C dec. MS [*m/e* (%, assignment(]: 480 (5, M^+), 452 (65, M^+ – CO), 396 (21, M^+ – 3CO), 368 (22, M^+ – 4CO), 340 (49, M^+ – 5CO), 312 (70, M^+ – 6CO), 284 (40, M^+ – 7CO), 256 (69, M^+ – 8CO), and smaller fragment ions.

$Fe(CO)_6$(FeCFCHCHCF) (4a): yellow crystals, mp 42 °C. MS [*m/e* (%, assignment)]: 368 (42, M^+), 340 (42, M^+ – CO), 312 (28, M^+ – 2CO), 284 (24, M^+ – 3CO), 256 (100, M^+ – 4CO), 228 (86, M^+ – 5CO), 200 (57, M^+ – 6 CO), and smaller fragment ions. ^{13}C NMR ($CDCl_3$): δ 83.9 (FeC*F*C*H*CHCF), ($^2J_{CF}$ = 14.6 Hz, $^3J_{CF}$ = 6.1 Hz), 213.7 (FeCFCHC*H*CF), ($^1J_{CF}$ = 361 Hz, $^4J_{CF}$ = 3.2 Hz), 208.1, 208.9 ($^3J_{CF}$ = 2Hz) (CO). The spectrum has been simulated using the LAOCN3 program.

$Fe(CO)_6$(FeCFCFCHCH) (5a): yellow crystals, mp 56–57 °C. MS [*m/e* (%, assignment)]: 368 (100, M^+), 340 (44, M^+ – CO), 312 (32, M^+ – 2CO), 284 (25, M^+ – 3CO), 256 (84, M^+ – 4CO), 228 (75, M^+ – 5CO), 200 (52, M^+ – 6 CO), and smaller fragment ions.

$Fe_2(CO)_8$(FeCFCCH$_3$CCH$_3$CF) (2b), $Fe_2(CO)_8$(FeCFCFC-CH$_3$CCH$_3$) (3b), $Fe(CO)_6$(FeCFCCH$_3$CCH$_3$CF) (4b), and Fe-$(CO)_6$(FeCFCFCCH$_3$CCH$_3$) (5b). $Fe_3(CO)_8(\mu_3\text{-CF})(\mu_3\text{-CFCCH}_3\text{CCH}_3)$ (**1b**) (125 mg, 0.25 mmol) was dissolved in 50 mL of *n*-hexane in a 100-mL glass vessel with a Teflon valve. The vessel was evacuated and the reaction mixture was kept at 80 °C for 2 days. To remove decomposition products, the solution was filtered through a layer of silica. Separation of the products has been performed using a medium-pressure liquid chromatography column (l = 65 cm, d = 3.5 cm; silica 60, 0.015–0.040 mm) using light petroleum (bp 40–60 °C) as eluant. The first yellow fraction contains **5b**, the second one **4b**, the third one **3b**, and the fourth one **2b**. Crystallization yields **2b** (20 mg, 0.04 mmol), **3b** (5 mg, 0.01 mmol), **4b** (12 mg, 0.03 mmol), and **5b** (1 mg, 0.002 mmol) impure, respectively.

$Fe_2(CO)_8$(FeCFCCH$_3$CCH$_3$CF) (2b): dark green crystals, mp 162 °C dec. MS [*m/e* (%, assignment)]: 508 (3, M^+), 480 (38, M^+ – CO), 452 (14, M^+ – 2CO), 424 (11, M^+ – 3CO), 396 (21, M^+ – 4CO), 368 (47, M^+ – 5CO), 340 (100, M^+ – 6CO), 312 (61, M^+ – 7CO), 284 (35, M^+ – 8CO), and smaller fragment ions.

$Fe_2(CO)_8$(FeCFCFCCH$_3$CCH$_3$) (3b): dark green crystals, mp 134 °C dec. MS [*m/e* (%, assignment)]: 508 (6, M^+), 480 (56, M^+ – CO), 424 (24, M^+ – 3CO), 368 (49, M^+ – 5CO), 340 (100, M^+ – 6CO), 312 (56, M^+ – 7CO), 284 (68, M^+ – 8CO), and smaller fragment ions.

$Fe(CO)_6$(FeCFCCH$_3$CCH$_3$CF) (4b): yellow crystals, mp 46–47 °C. MS [*m/e* (%, assignment)]: 396 (34, M^+), 368 (28 M^+ – CO), 340 (30, M^+ – 2CO), 312 (24, M^+ – 3CO), 284 (100, M^+ – 4CO), 256 (58, M^+ – 5CO), 228 (33, M^+ – 6CO), and smaller fragment ions.

$Fe_2(CO)_8$(FeCFCCH$_3$CC$_6$H$_5$CF) (2c), $Fe_2(CO)_8$(FeCFCFC-CH$_3$CC$_6$H$_5$) (3c), $Fe(CO)_6$(FeCFCCH$_3$CC$_6$H$_5$CF) (4c), and $Fe(CO)_6$(FeCFCFCCH$_3$CC$_6$H$_5$) (5c). $Fe_3(CO)_8(\mu_3\text{-CF})(\mu_3\text{-CFCCH}_3\text{CC}_6\text{H}_5)$ (**1c**) (247 mg, 0.43 mmol) was dissolved in a 100-mL glass vessel with a Teflon valve in 50 mL of *n*-hexane. The vessel was evacuated, and the reaction mixture was kept at 80 °C for 3 days. Separation of the products has been performed using a medium-pressure liquid chromatography column (l = 65 cm, d = 3.5 cm; silica 60, 0.015-0.040 mm) using light petroleum (bp 40–60 °C) as eluant. The separation of the yellow fraction is incomplete. It contains both compounds, **4c** and **5c**. Pure **5c** (30 mg, 0.07 mmol) has been obtained by crystallization from *n*-pentane at –78 °C. The remaining solution was evaporated to dryness. **4c** (10 mg, 0.02 mmol) contaminated with **5c** was isolated as a yellow oily liquid. The third fraction contains **3c**, and the fourth one, **2c**. Crystallization yields **2c** (9 mg, 0.016 mmol) and **3c** (6 mg, 0.011 mmol).

$Fe_2(CO)_8$(FeCFCCH$_3$CC$_6$H$_5$CF) (2c): dark green crystals, mp 140 °C. MS [*m/e* (%, assignment)]: 570 (1, M^+), 542 (28, M^+ – CO), 514 (16, M^+ – 2CO), 486 (11, M^+ – 3CO), 458 (18, M^+ – 4CO), 430 (42, M^+ – 5CO), 402 (69, M^+ – 6CO), 374 (55, M^+ – 7CO), 346 (28, M^+ - 8CO), and smaller fragment ions.

$Fe_2(CO)_8$(FeCFCFCCH$_3$CC$_6$H$_5$) (3c): dark green crystals, mp 127 °C. MS [*m/e* (%, assignment)]: 570 (30, M^+), 542 (78, M^+ – CO), 514 (40, M^+ – 2CO), 486 (74, M^+ – 3CO), 458 (94, M^+ – 4CO), 430 (88, M^+ – 5CO), 402 (57, M^+ – 6CO), 374 (86, M^+ – 7CO), 346 (97, M^+ – 8CO), and smaller fragment ions.

$Fe(CO)_6$(FeCFCFCCH$_3$CC$_6$H$_5$) (5c): yellow crystals, mp 97–99 °C. MS [*m/e* (%, assignment)]: 458 (18, M^+), 430 (40, M^+ – CO), 402 (47, M^+ – 2CO), 374 (52, M^+ – 3CO), 346 (93, M^+ – 4CO), 318 (100, M^+ – 5CO), 290 (64, M^+ - 6CO), and smaller fragment ions.

$Fe_2(CO)_8$(FeCFCHCCH$_3$CF) (2d) and $Fe(CO)_6$(FeCFCH-CCH$_3$CF) (4d). $Fe_3(CO)_8(\mu_3\text{-CF})(\mu_3\text{-CFCHCCH}_3)$ (**1d**) (45 mg, 0.091 mmol) was dissolved in *n*-hexane and sealed in a glass tube (4-mm outer diameter) under vacuum, and the contents were heated to 80 °C for 18 h. The reaction was monitored by ^{19}F NMR spectroscopy. Separation of the products has been performed by thin-layer chromatography eluting with light petroleum (bp 40–60 °C). The first yellow fraction contains **4d** as a yellow oil, and the second one contains **2d** (10 mg, 0.02 mmol). Sublimation under vacuum (25 °C, 10^{-2} mbar) onto a receiver kept at –40 °C yielded **4d** (7 mg, 0.02 mmol) as yellow crystals.

$Fe_2(CO)_8$(FeCFCHCCH$_3$CF) (2d): dark green crystals, mp 150 °C dec. MS [*m/e* (%, assignment)]: 494 (5, M^+), 466 (54, M^+ – CO), 438 (13, M^+ – 2CO), 410 (12, M^+ – 3CO), 382 (24, M^+ – 4CO), 354 (52, M^+ – 5CO), 326 (100, M^+ – 6CO), 298 (65, M^+ – 7CO), 270 (52, M^+ – 8CO), and smaller fragment ions.

$Fe(CO)_6$(FeCFCHCCH$_3$CF) (4d): yellow crystals, mp 41 °C. MS [*m/e* (%, assignment)]: 382 (28, M^+), 354 (31, M^+ – CO), 326 (26, M^+ – 2CO), 298 (22, M^+ – 3CO), 270 (100, M^+ – 4CO),

(12) Wade, K. *Adv. Inorg. Chem. Radiochem.* **1976**, *18*, 1.

(13) Bothner-By, A. A.; Castellano, S. M. LAOCN3 (A Program for Computer Simulation of Complex NMR Spectra. *In Computer Programs for Chemistry*; de Tar, D. F., Ed.; W. A. Benjamin, Inc.: New York, 1968; Vol. 1, Chapter 3. Clark, M.; Thrasher, J. S. MS-DOS Version for IBM Personal Computer. The University of Alabama, Tuscaloosa, AL.

Scheme I

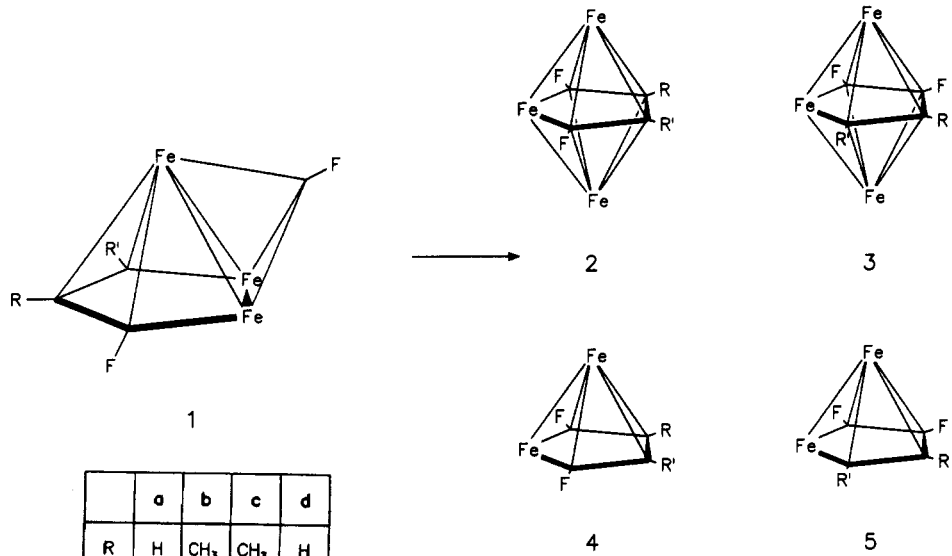

	a	b	c	d
R	H	CH_3	CH_3	H
R'	H	CH_3	C_6H_5	CH_3

242 (80, $M^+ - 5CO$), 214 (51, $M^+ - 6CO$), and smaller fragment ions.

X-ray Crystal Structure Determination of $Fe_2(CO)_8$(FeCFCHCHCF) (2a), $Fe_2(CO)_8$(FeCFCFCHCH) (3a), and $Fe_2(CO)_8$(FeCFCCH$_3$CC$_6$H$_5$CF) (2c). A suitable crystal (0.4 × 0.5 × 0.4 mm^3) of **2a**, obtained by slow cooling of a *n*-hexane/dichloromethane solution, was sealed in a glass capilary. A crystal (0.3 × 0.3 × 0.25 mm^3) of **3a**, obtained by slow cooling of a *n*-hexane/dichloromethane solution, was mounted on the top of a glass fiber. A needle-shaped crystal (0.375 × 0.075 × 0.005 mm^3) of **2c**, obtained by slow cooling of a *n*-hexane/dichloromethane solution, was mounted on the top of a glass fiber. The data were collected using a Stoe diffractometer for **2a** and **2c** and on Enraf-Nonius CAD4 diffractometer for **3a**. Data were reduced to structure factors by correction for Lorentz and polarization effects. The space groups *Pcab* (No. 61) for **2a**, $P2_1/c$ (No. 14) for **2c**, and *Pnma* (No. 62) for **3a** were uniquely defined by systematic absences. Empirical absorption corrections, DIFABS,[14] were applied. The structures were solved by direct methods, SHELXS 86.[15] Successive, difference Fourier maps and least-squares refinement cycles, SHELX 76,[16] revealed the positions of all atoms for **2a** and **3a** and all non-hydrogen atoms for **2c**, respectively. All non-hydrogen atoms were refined anisotropically and the hydrogen atoms isotropically with a fixed temperature factor (U = 0.05) for **2a** and **3a**. The structure of **2c** has been refined using isotropic temprature factors for the Fe, C, F, and O atoms. Molecular drawings have been obtained using the programs SCHAKAL88[17] and ORTEP.[18]

Results

The reactions of this work are summarized in Scheme I. The infrared and ^{1}H NMR spectroscopic data for the compounds are presented in Tables V and VI. X-ray crystal structure determinations were undertaken for $Fe_2(CO)_8$(FeCFCHCHCF) (**2a**), $Fe_2(CO)_8$(FeCFCFCHCH) (**3a**), and $Fe_2(CO)_8$(FeCFCCH$_3$CC$_6$H$_5$CF) (**2c**). The data are summarized in Table I. The final fractional atomic coordinates are listed in Tables II–IV for **2a**, **3a**, and **2c**, respectively. Important bond lengths and angles are summarized in Tables VII and VIII. The molecular structures and atom-numbering schemes are depicted in Figure 1–3.

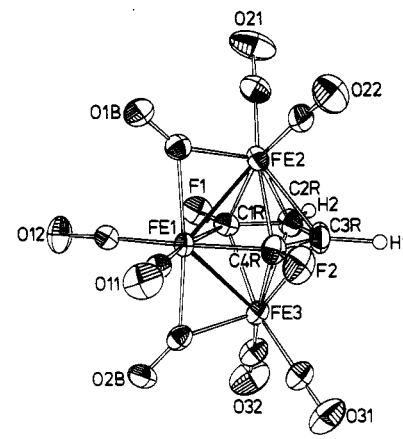

Figure 1. ORTEP plot of **2a**.

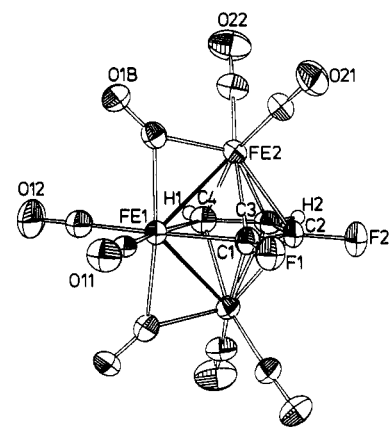

Figure 2. ORTEP plot of **3a**.

Discussion

Thermolysis of the diferraallyl clusters $Fe_3(CO)_8(\mu_3$-CF)(μ_3-CFCRCR′ (**1a–d**) (**a**, R = R′ = H; **b**, R = R′ = CH_3;

(14) Walker, N.; Stuart, D. *Acta Crystallogr. Sect. A* **1983**, *39*, 158.
(15) Sheldrick, G. M. SHELXS86, A Program for Crystal Structure Solution. Göttingen, 1986.
(16) Sheldrick, G. M. SHELX76, A Program for Crystal Structure Determination. Cambridge, 1976.
(17) Keller, E. SCHAKAL88, A FORTRAN Program for the Graphic Representation of Molecular and Crystallographic Models. Universität Freiburg, 1988.
(18) Johnson, C. K. ORTEP, A FORTRAN Thermal-Ellipsoid Plot Program for Crystal Structure Illustrations. Report ORNL-3794, Oak Ridge National Laboratories, Oak Ridge, TN.

Table I. Crystallographic Data for $Fe_2(CO)_8(FeCFCHCHCF)$ (2a), $Fe_2(CO)_8(FeCHCHCFCF)$ (3a), and $Fe_2(CO)_8(FeCFCCH_3CC_6H_5CF)$ (2c)

	2a	3a	2c
formula	$C_{12}H_2F_2Fe_3O_8$	$C_{12}H_2F_2Fe_3O_8$	$C_{19}H_8F_2Fe_3O_8$
fw	480	480	570
cryst size, mm^3	0.4 × 0.5 × 0.5	0.3 × 0.3 × 0.25	0.375 × 0.075 × 0.005
a, Å	11.416 (4)	11.524 (9)	18.214 (6)
b, Å	15.748 (4)	10.994 (9)	7.035 (3)
c, Å	16.129 (5)	11.42 (2)	17.845 (6)
β, deg			117.37 (3)
V, $Å^3$	2899.7	1446.9	2031.2
Z	8	4	4
cryst syst	orthorhombic	orthorhombic	monoclinic
space group	*Pcab* (No. 61)	*Pnma* (No. 62)	$P2_1/c$ (No. 14)
d_{calc}, g cm^{-3}	2.20	2.20	1.86
diffractometer	STOE	CAD4	STOE
monochromator	graphite	graphite	graphite
θ range, deg	$2 \le \theta \le 27$	$2 \le \theta \le 25$	$2 \le \theta \le 20$
h	$0 \le h \le 14$	$-13 \le h \le 4$	$-17 \le h \le 15$
k	$0 \le k \le 20$	$-13 \le k \le 0$	$0 \le k \le 6$
l	$0 \le l \le 20$	$-13 \le l \le 0$	$0 \le l \le 16$
λ, Å	0.710 69	0.710 69	0.710 69
μ, cm^{-1}	30.3	30.3	21.8
abs corr	empirical DIFABS[a]	empirical DIFABS[a]	empirical DIFABS[a]
temp factors	Fe, C, F, O anisotropic; H isotropic	Fe, C, F, O anisotropic; H isotropic	Fe anisotropic; C, F, O isotropic
no. of measd rflns	3562	2059	1933
no. of unique rflns	3157	1346	1845
no. of obsd rflns	2611 ($F_o > 3\sigma(F_o)$)	1155 ($F_o > 3\sigma(F_o)$)	855 ($F_o > 3\sigma(F_o)$)
no. of variables	233	134	144
$R(F_o)$	0.040	0.040	0.103
$R_w(F_o)$	0.040	0.041	0.080
w	$(\sigma^2(F_o) + 0.0005F_o^2)^{-1}$	$(\sigma^2(F_o) + 0.0005F_o^2)^{-1}$	$(\sigma^2(F_o) + 0.0005F_o^2)^{-1}$
Δ/σ	0.004	0.001	0.001
res electr dens, e $Å^{-3}$	0.51	0.73	1.03

[a] See ref 14.

Table II. Fractional Atomic Coordinates and Temperature Factors for 2a

atom	x	y	z	B_{eq}, $Å^2$
Fe1	0.1313 (1)	0.3566 (1)	0.3924 (1)	1.85
Fe2	0.2368 (1)	0.3391 (1)	0.2622 (1)	2.28
Fe3	0.2367 (1)	0.4892 (1)	0.4134 (1)	2.24
C1R	0.3038 (3)	0.3687 (2)	0.3809 (2)	2.27
C2R	0.3534 (4)	0.4277 (3)	0.3249 (3)	2.82
C3R	0.2651 (4)	0.4732 (3)	0.2816 (3)	3.06
C4R	0.1510 (3)	0.4459 (3)	0.3080 (2)	2.52
F1	0.3825 (2)	0.3220 (2)	0.4240 (2)	3.03
F2	0.0606 (3)	0.4863 (2)	0.2690 (2)	3.85
C11	−0.0256 (4)	0.3613 (2)	0.3888 (2)	2.55
C12	0.1344 (3)	0.2754 (3)	0.4694 (2)	2.62
O11	−0.1242 (2)	0.3664 (2)	0.3846 (2)	4.18
O12	0.1361 (3)	0.2252 (2)	0.5191 (2)	4.70
C1B	0.1358 (3)	0.2583 (3)	0.3049 (2)	2.65
C2B	0.1337 (3)	0.4424 (2)	0.4903 (3)	2.51
O1B	0.0954 (3)	0.1913 (2)	0.3006 (2)	3.83
O2B	0.0918 (3)	0.4457 (2)	0.5551 (2)	3.42
C21	0.3403 (4)	0.2635 (3)	0.2263 (3)	3.29
C22	0.1736 (4)	0.3457 (3)	0.1617 (3)	3.12
O21	0.4009 (3)	0.2110 (3)	0.2031 (2)	5.60
O22	0.1313 (4)	0.3529 (2)	0.0991 (2)	5.08
C31	0.1746 (4)	0.5919 (3)	0.4099 (3)	3.19
C32	0.3386 (4)	0.5228 (3)	0.4905 (3)	3.26
O31	0.1321 (3)	0.6570 (2)	0.4066 (3)	5.01
O32	0.3971 (3)	0.5437 (3)	0.5427 (3)	5.18
H1	0.275 (4)	0.518 (3)	0.239 (3)	3.95
H2	0.427 (4)	0.431 (3)	0.316 (3)	3.95

Table III. Fractional Atomic Coordinates and Temperature Factors for 3a

atom	x	y	z	B_{eq}, $Å^2$
Fe1	0.1293 (1)	0.7500	0.5418 (1)	1.94
Fe2	0.2376 (1)	0.5957 (1)	0.4351 (1)	2.18
C1R	0.1513 (5)	0.7500	0.3691 (5)	2.34
C2R	0.2648 (6)	0.7500	0.3213 (5)	2.55
C3R	0.3547 (6)	0.7500	0.4057 (6)	2.61
C4R	0.3063 (6)	0.7500	0.5208 (6)	2.43
F1	0.0620 (3)	0.7500	0.2903 (3)	3.12
F2	0.2831 (4)	0.7500	0.2047 (3)	3.83
C11	−0.0271 (6)	0.7500	0.5341 (5)	2.21
C12	0.1296 (6)	0.7500	0.6988 (6)	2.96
O11	−0.1245 (4)	0.7500	0.5290 (4)	3.45
O12	0.1261 (6)	0.7500	0.7964 (4)	5.16
C21	0.1828 (4)	0.4928 (4)	0.3281 (4)	2.75
C22	0.3392 (4)	0.4842 (4)	0.4846 (5)	3.23
C1B	0.1301 (4)	0.5612 (4)	0.5539 (4)	2.40
O21	0.3516 (3)	0.5698 (3)	0.7582 (3)	4.18
O22	0.3992 (4)	0.4102 (4)	0.5181 (4)	5.06
O1B	0.0864 (3)	0.4909 (3)	0.6123 (3)	3.33
H1	0.364 (7)	0.7500	0.573 (7)	3.95
H2	0.444 (7)	0.7500	0.376 (7)	3.95

c, R = CH_3, R′ = C_6H_5; **d**, R = H, R′ = CH_3) in hexane yields the isomeric trinuclear ferroles $Fe_2(CO)_8$(FeCFCRCR′CF) (**2a–d**) and $Fe_2(CO)_8$(FeCFCFCRCR′) (**3a–c**). In addition the corresponding dinuclear species $Fe(CO)_6$(FeCFCRCR′CF) (**4a–d**) and $Fe(CO)_6$(FeCFCFCRCR′) (**5a–c**), respectively, are obtained (Scheme I). The ratio of the isomers determined by ^{19}F NMR spectroscopy of the reaction mixture as well as the presence of some not fully characterized minor products depends somewhat on the reaction conditions, mainly on the volume of the reactor. The four major products **2–5** have been separated by chromatography (although incomplete for **4b,c** and **5b,c**) and characterized by spectroscopic methods (Tables V and VI) and X-ray crystallography (Tables I–III, VII, and VIII; Figures 1–3) for **2a**, **3a**, and **2c**.

The closo clusters **2** and **3** consist of pentagonal bipyramids. The mass spectra of the two isomers are rather similar, showing the molecular ion and smaller fragment ions by successive loss of eight carbonyl ligands. Bands around 1870 cm^{-1} in the infrared spectra (Table V) clearly indicate the presence of bridging carbonyl ligands. More informative, however, are the ^{19}F NMR and ^1H NMR spectra (Table V) of these compounds. In **2** the fluorine

Table IV. Fractional Atomic Coordinates and Temperature Factors for 2c

atom	x	y	z	B_{eq}, Å^2
Fe1	0.8240 (3)	0.0093 (9)	0.6072 (3)	3.01
Fe2	0.6837 (3)	−0.0911 (8)	0.5682 (3)	1.98
Fe3	0.8470 (3)	0.0418 (9)	0.7517 (3)	2.37
C1R	0.7458 (20)	0.1426 (63)	0.6402 (21)	3.56
C2R	0.7138 (16)	0.0387 (52)	0.6871 (16)	1.73
C3R	0.7385 (18)	−0.1597 (55)	0.7058 (19)	2.80
C4R	0.7964 (20)	−0.1778 (62)	0.6707 (21)	3.87
C201	0.6601 (17)	0.1356 (50)	0.7227 (18)	2.42
C202	0.5914 (18)	0.2329 (55)	0.6665 (19)	3.51
C203	0.5360 (17)	0.3189 (52)	0.6940 (19)	3.12
C204	0.5579 (19)	0.2986 (59)	0.7840 (22)	4.33
C205	0.6255 (20)	0.1868 (55)	0.8354 (19)	3.94
C206	0.6779 (16)	0.1054 (49)	0.8072 (18)	2.44
C301	0.7140 (17)	−0.3123 (50)	0.7445 (18)	2.38
C1B	0.7365 (19)	−0.0775 (63)	0.4979 (22)	5.10
O1B	0.7270 (14)	−0.1393 (40)	0.4316 (15)	6.02
C2B	0.9257 (19)	0.1075 (59)	0.7198 (19)	3.81
O2B	0.9911 (14)	0.1555 (33)	0.7337 (13)	3.76
C11	0.8955 (21)	−0.1233 (60)	0.5893 (21)	4.70
O11	0.9363 (14)	−0.2275 (42)	0.5727 (14)	5.61
C12	0.8344 (20)	0.2001 (65)	0.5565 (21)	4.53
O12	0.8399 (15)	0.3389 (45)	0.5217 (16)	6.66
C21	0.5964 (19)	0.0353 (57)	0.4996 (19)	3.60
O21	0.5397 (12)	0.1192 (37)	0.4518 (12)	3.92
C22	0.6324 (21)	−0.3110 (63)	0.5313 (21)	4.15
O22	0.5897 (15)	−0.4406 (43)	0.5097 (14)	5.68
C31	0.9093 (20)	−0.0926 (59)	0.8383 (21)	4.12
O31	0.9526 (15)	−0.1669 (42)	0.8982 (16)	6.62
C32	0.8653 (20)	0.2379 (64)	0.8152 (21)	3.88
O32	0.8696 (12)	0.3672 (38)	0.8553 (13)	3.96
F1	0.7266 (10)	0.3199 (30)	0.6245 (10)	3.26
F2	0.8235 (10)	−0.3595 (32)	0.6799 (11)	4.57

substituents occupy the 2 and 5 positions of the ferrole ring. Consequently the ^{19}F NMR spectra of **2a,b** exhibit only one signal for the chemically equivalent fluorine atoms. These signals are observed at low field around −100 ppm. **2c** and **2d** have two signals in a similar chemical shift region indicating that the two fluorine atoms are in an α position with respect to the iron atom of the ferrole ring in accordance with the result of an X-ray crystal structure

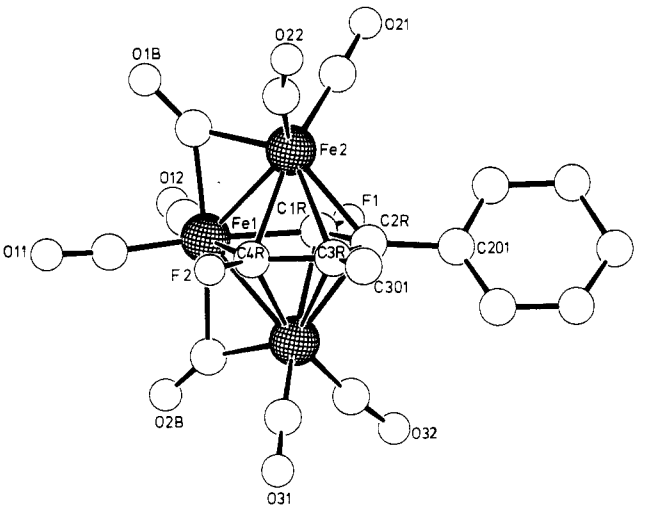

Figure 3. SCHAKAL plot of **2c**.

analysis of **2c**. The isomeric compounds **3** all exhibit two signals in the ^{19}F NMR spectra. Thus, the two fluorine atoms are nonequivalent. The chemical shift values of the low-field signal are very close to that observed for the isomers **2**, indicating that these fluorine atoms are in position 2 of the ferrole ring, the α position. The other signal is observed about 20 ppm high field, indicating that these fluorine atoms are in the β position. This would allow the fluorine substituent being in position 3 or 4 of the ferrole ring, respectively. Having the fluorine in position 4 would require splitting of the carbon–carbon bond between RC–CR′ of the diferraallyl ligand and reformation of all bonds. However, this would make it difficult to understand why only two isomers are formed. In addition, the β-fluorine atom in position 4 of **3b** would have two methyl groups at adjacent carbon atoms, which should result in a splitting of these signal into a quartet of a quartet, and the fluorine atom in the position 2 should be split in a quartet, too. However, the high-field signal of **3b** is split only into a doublet of a quartet, whereas the

Table V. Spectroscopic Data for the Compounds 2a–d and 3a–c

IR,[a] cm^{-1}	^{1}H NMR,[b] ppm	^{19}F NMR,[b] ppm
	$Fe_2(CO)_8(FeCFCHCHCF)$ (**2a**)	
2079 (w), 2036 (vs), 2013 (s), 1998 (s), 1878 (m)	aa′xx′ pattern, 6.91 (CFC*H*C*H*CF) ($^3J_{HH}$ = 1.2, $^4J_{HF}$ = 1.7, $^3J_{HF}$ = 7.0)	aa′xx′ pattern, −100.6 (C*F*CHCHC*F*) ($^4J_{FF}$ = 0.4 Hz)
	$Fe_2(CO)_8(FeCFCCH_3CCH_3CF)$ (**2b**)	
2073 (w), 2030 (vs), 2008 (s), 1987 (m), 1933 (w), 1871 (w)	3.13 ($^4J_{HF}$ = 1)	−105.24
	$Fe_2(CO)_8(FeCFCCH_3CC_6H_5CF)$ (**2c**)	
2087 (m), 2075 (s), 2046 (s), 2035 (vs), 1994 (s), 1988 (m), 1887 (m), 1877 (m)	2.99 (C*H*$_3$, $^4J_{HF}$ = 1.8), 7.84 (C$_6$*H*$_5$)	−101.5, −106.7
	$Fe_2(CO)_8(FeCFCHCCH_3CF)$ (**2d**)	
2076 (w), 2032 (vs), 2013 (m), 1992 (m), 1876 (w)	2.98 (C*H*$_3$, $^4J_{HF}$ = 1.2), 7.26 (C*H*, $^4J_{HH}$ = 1.7, $^3J_{HF}$ = 7.8)	−101.2, −105.6
	$Fe_2(CO)_8(FeCFCFCHCH)$ (**3a**)	
2076 (w), 2034 (vs), 2008 (vs), 2000 (s), 1869 (m)	abxy pattern, 1.39 (FeCFCFCHC*H*) ($^3J_{HH}$ = 5.7, $^4J_{HF}$ = 3.8, $^5J_{HF}$ = 0.9), 7.68 (FeCFCFC*H*CH) ($^4J_{HF}$ = 0.9, $^3J_{HF}$ = 4.6)	abxy pattern, −127.5 (FeC*F*CFCHCH), −147.5 (FeCFC*F*CHCH) ($^3J_{FF}$ = 19.4)
	$Fe_2(CO)_8(FeCFCFCCH_3CCH_3)$ (**3b**)	
2054 (w), 2124 (w), 2029 (vs), 2002 (s), 1988 (m), 1933 (w), 1872 (w)	3.25 (FeCFCFCC*H*$_3$CCH$_3$) ($^4J_{HF}$ = 1.2)	−128.3 (FeC*F*CFCCH$_3$CCH$_3$), −144.6 (FeCFC*F*CCH$_3$CCH$_3$) ($^3J_{FF}$ = 22)
	$Fe_2(CO)_8(FeCFCFCCH_3CC_6H_5)$ (**3c**)	
2071 (w), 2031 (vs), 2006 (m), 1999 (m), 1992 (m), 1874 (w)	3.1 (C*H*$_3$) ($^4J_{HF}$ = 1.2), 7.04 (C$_6$*H*$_5$)	−124.4 (FeC*F*CFCCH$_3$CC$_6$H$_5$), −145.0 (FeCFC*F*CCH$_3$CC$_6$H$_5$) ($^4J_{HF}$ = 1.2)

[a] Solutions in dichloromethane. [b] Solutions in $CDCl_3$ (**2a**) and CD_2Cl_2 (**2b–d**, **3a–c**). *J* values are in Hz.

Table VI. Spectroscopic Data for the Compounds 4a–d and 5a–c

IR,[a] cm^{-1}	^1H NMR,[b] ppm	^{19}F NMR,[b] ppm
	$Fe(CO)_6(FeCFCHCHCF)$ (**4a**)	
2092 (m), 2052 (vs), 2029 (s), 2015 (m)	aa'xx' pattern, 5.31 ($FeCFCHCHCF$) ($^3J_{HH}$ = 3.8) ($^3J_{HF}$ = 9.2)	aa'xx' pattern, −51.4 ($FeCFCHCHCF$) ($^4J_{FF}$ = 3.2) ($^4J_{HF}$ = 2.7)
	$Fe(CO)_6(FeCFCCH_3CCH_3CF)$ (**4b**)	
2087 (vs), 2045 (vs), 2025 (vs), 2006 (vs), 1998 (s), 1961 (m)	2.06 ($FeCFCCH_3CCH_3CF$)	−63.8 ($FeCFCCH_3CCH_3CF$)
	$Fe(CO)_6(FeCFCCH_3CC_6H_5CF)$ (**4c**)	
		−57.7 ($FeCFCCH_3CC_6H_5CF$), −63.8 ($FeCFCCH_3CC_6H_5CF$)
	$Fe(CO)_6(FeCFCHCCH_3CF)$ (**4d**)	
1968 (w), 2000 (m), 2027 (vs), 2048 (vs), 2089 (vs), 2100 (vs)	5.37 ($FeCFCHCCH_3CF$) ($^3J_{HF}$ = 9.3), 2.06 ($FeCFCHCH_3CF$) ($^4J_{HF}$ = 1.2)	−54.2 ($FeCFCHCCH_3CF$), −62.7 ($FeCFCHCCH_3CF$) ($^4J_{FF}$ = 4.6)
	$Fe(CO)_6(FeCFCFCHCH)$ (**5a**)	
2089 (s), 2051 (vs), 2021 (vs), 2009 (vs), 1969 (m)	abxy pattern, 6.25 ($FeCFCFCHCH$) ($^3J_{HH}$ = 6.0, $^4J_{HF}$ = 6), 6.04 ($FeCFCFCHCH$) ($^3J_{HF}$ = 2.4, $^4J_{HF}$ = 2.9)	abxy pattern, −85.6 ($FeCFCFCHCH$) ($^4J_{HF}$ = 2.9, $^3J_{FF}$ = 16), −143.0 ($FeCFCFCHCH$) ($^4J_{HF}$ = 6.0, $^3J_{HF}$ = 2.4)
	$Fe(CO)_6(FeCFCFCCH_3CCH_3)$ (**5b**)	
		−91.5 ($FeCFCFCCH_3CCH_3$), −140.3 ($FeCFCFCCH_3CCH_3$)
	$Fe(CO)_6(FeCFCFCCH_3CC_6H_5)$ (**5c**)	
	2.03 ($FeCFCFCCH_3CC_6H_5$) ($^4J_{HF}$ = 1.5), 7.19 ($FeCFCFCCH_3CC_6H_5$)	−89.07, −89.30 ($FeCFCFCCH_3CC_6H_5$), −139.74, −139.92 ($FeCFCFCCH_3CC_6H_5$) ($^3J_{FF}$ = 19.5)

[a] Solutions in *n*-pentane. [b] Solutions in $CDCl_3$. *J* values are in Hz.

Table VII. Important Bond Lengths (Å) with Estimated Standard Deviations in Parentheses for $Fe_2(CO)_6(FeCFCHCHCF)$ (2a), $Fe_2(CO)_6(FeCFCCH_3CC_6H_5CF)$ (2c), and $Fe_2(CO)_6(CFCFCHCH)$ (3a)

	2a	2c	3a
Fe1–Fe2	2.436 (1)	2.425 (6)	2.433 (1)
Fe1–Fe3	2.433 (1)	2.426 (6)	
Fe1–C1R	1.986 (4)	2.01 (4)	1.988 (6)
Fe1–C4R	1.971 (4)	1.95 (4)	2.054 (7)
Fe1–C1B	2.097 (4)	1.97 (4)	2.081 (5)
Fe1–C2B	2.078 (4)	2.13 (3)	
Fe2–C1R	2.114 (4)	2.07 (4)	2.106 (4)
Fe2–C2R	2.177 (4)	2.14 (3)	2.160 (4)
Fe2–C3R	2.158 (4)	2.24 (4)	2.193 (4)
Fe2–C4R	2.081 (4)	2.12 (4)	2.113 (4)
Fe2–C1B	1.850 (4)	1.90 (4)	1.876 (5)
Fe3–C1R	2.112 (4)	2.12 (4)	
Fe3–C2R	2.179 (4)	2.16 (3)	
Fe3–C3R	2.166 94)	2.26 (4)	
Fe3–C4R	2.078 (4)	2.03 (4)	
Fe3–C2B	1.860 (4)	1.83 (4)	
C1R–C2R	1.414 (6)	1.42 (4)	1.418 (8)
C2R–C3R	1.420 (6)	1.45 (5)	1.414 (9)
C3R–C4R	1.436 (6)	1.46 (4)	1.427 (9)
C1R–F1	1.353 (4)	1.29 (4)	
C4R–F2	1.365 (4)	1.35 (4)	
C2R–F2			1.348 (7)

Table VIII. Important Bond Angles (deg) with Estimated Standard Deviations in Parentheses for $Fe_2(CO)_6(FeCFCHCHCF)$ (2a), $Fe_2(CO)_6(FeCFCCH_3CC_6H_5CF)$ (2c), and $Fe_2(CO)_6(FeCFCFCHCH)$ (3a)

	2a	2c	3a
Fe2–Fe1–Fe3(Fe2)	88.4 (1)	88.8 (2)	88.4 (1)
C1R–Fe1–C4R	75.8 (2)	74 (2)	76.0 (3)
Fe1–C1R–C2R	121.3 (3)	118 (3)	120.0 (4)
Fe1–C1R–F1	123.9 (3)	122 (3)	123.9 (4)
Fe2–C1R–Fe3(Fe2)	107.0 (2)	109 (1)	107.3 (3)
C1R–C2R–C3R	111.2 (3)	118 (2)	114.4 (5)
Fe2–C2R–Fe3(Fe2)	102.4 (2)	105 (1)	103.5 (2)
C2R–C3R–C4R	110.3 (3)	100 (3)	110.0 (6)
Fe2–C3R–Fe3(Fe2)	103.5 (2)	97 (1)	101.3 (3)
Fe1–C4R–C3R	121.4 (3)	129 (3)	119.7 (5)
Fe1–C4R–F2	124.4 (3)	121 (3)	
Fe2–C4R–Fe3	109.5 (2)	110 (2)	106.8 (3)

low-field signal exhibits a splitting into a doublet. Thus, we can conclude that the compounds **3** have the structures shown in Scheme I with the fluorine atoms in positions 2 and 3 in accordance with the result of the crystal structure determination of **3a**.

The ^{19}F NMR spectra of the compounds **2–5** clearly indicate that the low-field signals have to be assigned to the fluorine atoms in the α position in the ferrole ring. However, a different trend is observed in the ^1H NMR spectra of **2a** and **3a**, respectively. As the structures of **2a** and **3a** have been elucidated by X-ray crystallography, there is no doubt about their structures. The protons in β positions exhibit their resonances in the ^1H NMR spectra at 6.91 and 7.68 ppm for **2a** and **3a**, respectively. This is in accordance with literature data.[9] Again in accordance with literature data[9] the resonance of the α-hydrogen atom of **3a** is observed at high field at 1.39 ppm. Thus, the chemical shifts in ^1H and ^{19}F NMR spectra show just the opposite trends depending on the position at the ferrole ring.

Even more puzzling is the fact that in the dinuclear ferroles **4a** and **5a** the resonances of the α and β positions show very similar chemical shift values in the ^1H NMR spectra, whereas in the ^{19}F NMR spectra the same trend is observed as for the trinuclear cluster compounds **2** and **3**.

The same arguments in assigning the structures made for **2** and **3** hold for **4** and **5** as well. In addition, ^{13}C NMR data are available for some of these compounds due to their much higher solubility. The resonance of the α carbon atom of **2a** is observed at very low field, 213.7 ppm, exhibiting a large $^1J_{CF}$ coupling constant of 361 Hz. The signal of the β carbon atom is observed at 83.9 ppm for **2a**.

In all of these compounds the isomer formed by carbon–carbon bond formation at the nonfluorinated carbon atom is the prevailing one, especially for the dinuclear compounds **4** and **5**. However, an exact determination of the ratios of **2–5** by integrating the ^{19}F NMR spectra has been hindered by the presence of paramagnetic decomposition products and the much lower solubilities of **2** and **3** compared to **4** and **5** in hydrocarbon solvents. The

carbon–carbon bond formation occurs exclusively at the nonfluorinated carbon atom for the substituents H and CH_3, **1d**. Heating of **2b** and **3b** in *n*-hexane in a sealed NMR tube to 90 °C for 3 days results only in slow decomposition into the dinuclear cluster species **4b** and **5b**, respectively. No tendency of interconversion of **2** and **3** could be observed. In addition, no products from scrambling of the C_4 chain could be detected. From our data it is not possible to conclude which of the isomers **2** or **3** and **4** or **5** is the thermodynamically more stable one.

Crystal Structure Determinations. The crystals of the compounds **2a**, **3a**, and **2c** are built up by discrete molecules which do not show any unusual intermolecular distances. All of them possess a pentagonal bipyramidal cluster framework with one iron and four carbon atoms forming the pentagonal plane and two iron atoms forming the apices. The cluster framework is very similar to that of $Fe_2(CO)_8$(FeCPhCPhCPhCPh), which has been the first trinuclear ferrole structurally characterized.[19] The five atoms of the ferrole ring system as well as the direct substituents and the carbonyl ligands C11 and C12 are all almost in one plane. This plane even is a crystallographic mirror plane for **3a**, which has only half a molecule in the asymmetric unit. The Fe–Fe bonds have equal lengths within esd's. Carbon–carbon bond distances within the ferrole ring are very similar, ranging from 1.414 (6) to 1.436 (6) Å for **2a** and **3a**. These distances are close to that found in cyclopentadienyl rings indicating the delocalized π-system of the ferrole ring. The symmetrical isomer **2a** has both fluorine substituents in the α position with respect to the iron atoms and the hydrogen atoms in the β position, whereas in the asymmetric isomer **3a** the fluorine and hydrogen substituents occupy adjacent α and β positions, respectively. The major difference in bond length between isomers **2a** and **3a** is found in the Fe1–C bonds to the α carbon atoms C1 and C4, respectively. The Fe1–C bond to the nonfluorinated carbon atom C4 of 2.054 (7) Å is about 0.06 Å longer than the corresponding Fe1–C bond to the fluorinated carbon atoms, which range from 1.971 (4) to 1.988 (6) Å for **2a** and **3a**. This reflects a stronger metal to carbon bond for the fluorinated organometallic compound. A similar trend has been observed for other fluorinated organometallic compounds where data for comparison are available.[20] $Fe_3(CO)_8(\mu_3\text{-}CF)(\mu_3\text{-}CFCHCOC_2H_5)$[10] has Fe–C distances of 1.959 (5) and 2.015 (5) Å from the fluorinated and nonfluorinated terminal carbon atoms of the C_3 unit to the corresponding iron atoms. The Fe2–C distances of **2a** and **3a** show less striking differences. However, these differences are not as large as the one observed for Fe1. In all of these compounds each iron atom possesses two terminal carbonyl ligands. The two remaining carbonyl ligands form strongly asymmetric bridges between Fe1, Fe2, and Fe3, respectively. The Fe–C distances of these bridges to Fe2 and Fe3 are found about 0.2–0.25 Å shorter than the one to Fe1. The quality of the crystal of **2c** has been not as good as for **2a** and **3a**. Thus, the X-ray crystallographic data show much larger estimated standard deviations. However, one can see that the aromatic ring is turned out of the plane of the ferrole ring.

Conclusion. Due to the high regioselectivity of the reaction of $Fe_3(CO)_9(\mu_3\text{-}CF)_2$ with alkynes[10] and the thermal rearrangement of the resulting diferraallyl clusters into ferrole clusters, this reaction sequence is an optimized method for the systematic buildup of fluorinated ferrole cluster frameworks with substituents in well-defined positions. This reaction reflects the influence of iron–carbon bond strength on the product distribution. The products which require splitting of the shorter (stronger) metal–carbon bond, the Fe–C bond to the fluorinated carbon atom of the C_3 chain, are less abundant.

Acknowledgment. This research was supported by the Deutsche Forschungsgemeinschaft and the Fonds der Chemischen Industrie. We acknowledge Prof. Dr. J. Fuchs and I. Brüdgam for their assistance in the crystallographic work.

Supplementary Material Available: Tables listing crystallographic details, anisotropic temperature factors, interatomic distances, and interatomic angles for **2a**, **3a**, and **2c** (10 pages). Ordering information is given on any current masthead page.

OM9201526

(19) Dodge, R. P.; Schomaker, V. *J. Organomet. Chem.* **1965**, *3*, 274. Hock, A. A.; Mills, O. S. *Acta Crystallogr., Sect. A* **1961**, *14*, 139.

(20) Guggenberger, L. J.; Cramer, R. *J. Am. Chem. Soc.* **1972**, *94*, 3779. Hughes, R. P. *Adv. Organomet. Chem.* **1990**, *31*, 183.